Biological and Medical Applications of Materials and Interfaces

Facile solvothermal preparation of Mn2CuO4 microspheres: Excellent electrocatalyst for real-time detection of H2O2 released from live cells

Paramasivam Balasubramanian, Muthaiah Annalakshmi, Shen-Ming Chen, Tamilarasan Sathesh, Tie-Kun Peng, and TST Balamurugan

ACS Appl. Mater. Interfaces, **Just Accepted Manuscript** • DOI: 10.1021/acsami.8b18510 • Publication Date (Web): 29 Nov 2018

Facile solvothermal preparation of Mn_2CuO_4 microspheres: Excellent electrocatalyst for real-time detection of H_2O_2 released from live cells

Paramasivam Balasubramanian[1], Muthaiah Annalakshmi[1], Shen-Ming Chen[1]*, Tamilarasan Sathesh[2], Tie-Kun Peng[3], T.S.T. Balamurugan[1,3]

[1]Department of Chemical Engineering and Biotechnology, National Taipei University of Technology, No.1, Section 3, Chung-Hsiao East Road, Taipei 106, Taiwan, ROC.

[2]Department of Energy and Refrigerating Air-conditioning engineering, National Taipei University of Technology, Taipei 106, Taiwan, ROC.

[3]Institute of Biochemical and Biomedical Engineering, National Taipei University of Technology, No.1, Section 3, Chung-Hsiao East Road, Taipei 106, Taiwan, ROC.

ABSTRACT

Hydrogen peroxide (H_2O_2) is an eminent biomarker in pathogenesis; a selective, high sensitive real-time detection of H_2O_2 released from live cells have drawn a significant research interest in bio-analytical chemistry. Binary transition metal oxides (BTMOs) displayed the recognizable benefit in enhancing the sensitivity of H_2O_2 detection, though reported BTMOs based H_2O_2 sensor's detection limit is still insufficient, is not appropriate for *in-situ* profiling of trace amounts of cellular H_2O_2. In this, we describe an efficient, reliable electrochemical biosensor based on Mn_2CuO_4 microspheres to assay cellular H_2O_2. The Mn_2CuO_4 microspheres were prepared through a superficial solvothermal method. It is obvious from impedance studies, introduction of manganese into copper oxide lattice significantly improved the ionic conductivity, which is beneficial for electrochemical sensing process. Thanks to the distinct microsphere structure and excellent synergy; MCO modified electrode exhibited excellent nonenzymatic electrochemical behavior toward H_2O_2 sensing. The MCO modified electrode delivered a broad working range (36 nM to 9.3 mM) appreciable detection limit (13 nM), with high selectivity towards H_2O_2. To prove its practicality, the developed sensor was applied in the detection of cellular H_2O_2 release by Raw 264.7 cells in presence of CHAPS. These results label the possible appliance of the sensor in clinical analysis, and pathophysiology. Thus, BTMOs are evolving as a promising candidate in designing catalytic matrices for biosensor applications.

Keywords: reactive oxygen species (ROS); H_2O_2; manganese copper oxide; electrocatalysis; electrochemical sensor.

INTRODUCTION

Hydrogen peroxide (H_2O_2), a renowned reactive oxygen species (ROS),and bi product of cellular metabolism; which plays a crucial role in physiological process.[1] It has been extensively used in food, textile and paper industry, pharmaceutical formulation, clinical analysis, mining, and chemical industries.[2] In biological system, adequate amount of H_2O_2 (1-700 nM) is essential for intracellular signal transduction, cell proliferation, protein synthesis and controlling the living activities.[3] When the concentration of H_2O_2 is exceeding the permissible limit (>700 nM) is associates with the cell damage, oxidative stress, diabetes, cardiovascular diseases, welcoming the series of diseases, arteriosclerosis, Alzheimer's disease, cancer and so on.[4,5] As per literature, a higher concentration of H_2O_2 is produced from cancer cells due to the abnormal growth of tumor, which are rapidly elevates the level of H_2O_2 in biological system.[6] Therefore, the precise and reliable detection of endogenous H_2O_2 becoming an interesting research topic to diagnosis and treat the cancer and other diseases, thus the H_2O_2 can be identified as a tumor biomarker.[5] In this fact, a number of protocols have been reported to H_2O_2 assay, including colorimetric,[7] chemiluminescence,[8] high performance liquid chromatography,[9] fluorescence[10] and electrochemical sensors.[11,12,13] Amongst, electrochemical sensing strategy have received much more research interest owing to their fascinating features such as rapidity, accuracy, portability, economical, high sensitivity and selectivity, capability for *in-situ* H_2O_2 sensing.[14]

Nowadays, non-enzymatic H_2O_2 sensors have gained a dramatic attention in practical application than the enzymatic sensors courtesy of its rapid assay performance, high sensitivity, stability, and ease of operation; but enzyme-based sensors can simply mislay their activity caused by denaturation.[15,16,17,18] In this regard, a series of nanomaterial-based enzymeless sensors were reported for the sensing of extra-cellular H_2O_2.[2,19,20,21,22,23] Usually, living cells are secreted the H_2O_2 in nanomolar range but these modified electrode-based sensors does not achieve the sufficient detection limit and the synthesis method of electrode materials involves complex procedure and laborious is still hampered their widespread commercialization.[11] Therefore, the development of innovative and fascinating nanomaterials based sensitive assay system that allows

to assay the trace of cellular H_2O_2 release is necessary in the field of medical diagnosis as well as environmental production and food safety.[2]

Recent decades, an extensive research interest is devoted on the synthesis of binary transition metal oxides (BTMOs) thanks to their high earth abundance, non-toxic, low-cost, and superior redox behavior; coupled with exclusive electrocatalytic properties for a range of electrochemical utilities such energy storage, and conversion devices.[24,25] It should be noted that these BTMOs are exhibited an enhanced electrochemical conductance and high specific surface area over the uni-metal oxides, the presence of multi valent cations moderately reduce activation energy for the electron transfer process, the close bonding and synergetic coupling effects the two cations.[25,26] Thus, BTMOs are evolving as auspicious and attractive electrode materials for electrochemical sensing application.[27] For instance, Vasuki et al., have described the template-assisted preparation of hollow nanostructured $CoFe_2O_4$ for the determination of H_2O_2, it has been shown that $CoFe_2O_4$/GCE show very a low detection limit and broad dynamic range over Fe_3O_4/GCE.[28] Liu et al., fabricated a novel H_2O_2 sensor based on cubic-shaped $CoMn_2O_4$ nanoparticles and achieved an improved electrochemical performance.[29] Wu et al., synthesized the flake-like Mn_3O_4-$MnCo_2O_4$ nanoparticles by using CNTs as the sacrificial template, as-synthesized BTMOs modified electrode shows elevated electrocatalytic towards the detection of H_2O_2.[26] Shu et al., concluded that cube-like $CoSn(OH)_6$ nanostructure modified electrode also gave a superior electrocatalysis for H_2O_2 sensing.[30] It can be concluded that BTMOs has significantly improved electrocatalytic sensing behaviour towards the detection of H_2O_2 than that of pure metal oxides because insertion of second metal into monometal oxide catalyst, can alter the morphology, and electronic structure with superb synergy.[31] Also, this enriched electrochemical behaviour of BTMOs towards the H_2O_2 sensing caused by the existence of multiple valence of the two different cations in such BTMOs, which provide donor-acceptor active sites for the reversible adsorption of oxygen (H_2O_2).[25]

Many reports available on the copper oxide based H_2O_2 sensors, including Cu@CuO,[32] CuO/Ag,[33] CuO,[34] CuO-ionic liquid,[35] CuO nanoflowers,[36] CuO microcubes.[37] Nonetheless these electrodes do not achieve the sufficient detection limit, working range, and durability because of intrinsically poor electronic conductivity, and insufficient electrocatalysis of CuO. It is well known that doping the second metal into CuO can generates synergistic effects and would be expected to

boost the electrochemical performance compared with pure CuO via lowering the charge transfer resistance and offer enlarged reactive active sites. However, to the best of our knowledge, no literature available on the synthesis of Mn doped CuO and its electrochemical sensing application, until now.

Inspired by this at present, we state an efficient production of Mn_2CuO_4 (MCO) microspheres via facile solvothermal coupled low temperature calcination protocol. Further, as-synthesized MCO was utilized as an electrode modifier to create a novel, highly sensitive and selective nonenzymatic H_2O_2 biosensor. The electrocatalytic sensing studies validate that the MCO microspheres holds brilliant electrochemical performance for H_2O_2 sensing. The possible analytical application of the developed sensor has also been explored by monitoring endogenous H_2O_2 concentration secreted from live cells. The synthesis of MCO and electrochemical sensing of H_2O_2 is shown in Scheme. 1.

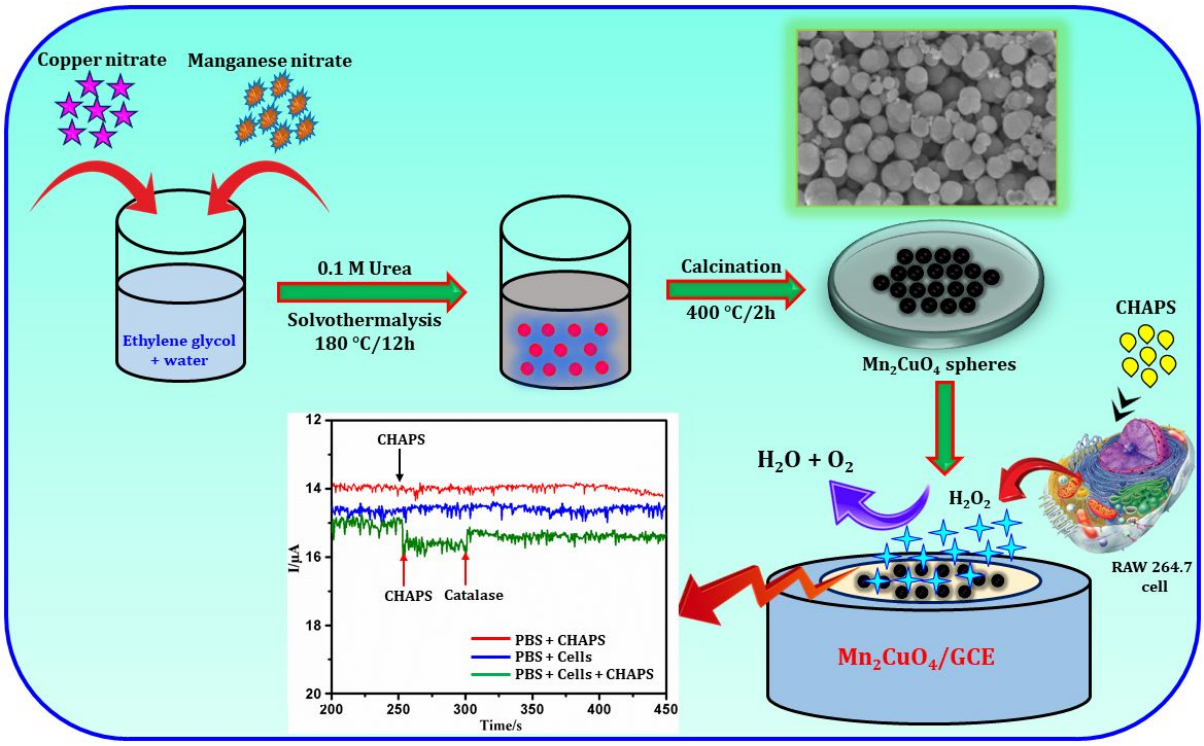

Scheme. 1. A pictographic model of the MCO synthesis and proposed MCO/GCE assay for endogenous H_2O_2 produced by Raw 264.7 cells.

EXPERIMENTAL

Synthesis of Mn_2CuO_4 microspheres

The synthesis of Mn_2CuO_4 (MCO) microspheres are based on a hydrothermal process, followed by the calcination. Typically, 0.05 M copper nitrate (10 mL) and 0.025 M manganese nitrate (10 mL) were added to 40 mL solvent (1:3 ratio of ethylene glycol, and DIW) under constant stirring at room temperature. Secondly, 10 mL of 0.1 M urea was gradually into the above mixture and vigorously stirred until get a complete dissolution. After that, the reaction mixture was poured into a 100 mL Teflon-lined steel autoclave and kept at 180 °C for 12h. After completion of solvothermalysis, the sample was collected by centrifugation and thoroughly cleansed with DIW and ethanol to remove unreacted substances, and allowed to drying at 60 °C overnight. To obtain Mn_2CuO_4 microspheres, as-prepared precursor sample was annealed at 400 °C for 2h in air.

RESULTS AND DISCUSSION

Material characterization

The surface morphological structure of MCO were studied by TEM. As depicted in Fig. 1a, MCO reveal sphere-like morphologies and these microspheres are appearing with a uniform size have an average diameter of ~1.3 μm. High magnified TEM image (Fig. 2b) obviously demonstrate the spherical microstructure of MCO, possesses a relatively thick and rough surface structure, which is beneficial to enrich the number of diffusion of analytes during the electrochemical sensing process.[38] Fig. 1c shows the HRTEM image of region marked by the green dash square of Fig. 1b, calculated interplanar distance is 0.479, 0.293, and 0.250 nm, matching with the (111), (220), and (311) lattice planes of Mn_2CuO_4, indicate that MCO microspheres are well-crystallized. Besides, Fig. 1d displays the corresponding SAED patterns, received patterns indexed with (111), (220), (311), (222), and (400) crystal planes of cubic Mn_2CuO_4 phase ([FM3-M]-Space group 227), as depicted in Fig. 1d, is in correlation with the results of X-ray diffraction studies. This results further verifies the high crystalline nature of MCO microspheres. Energy dispersive X-ray spectroscopy was employed to find out the chemical composition of MCO microspheres and displayed in Fig. 1e&f. As illustrated in Fig. 1e, elemental peaks observed for Cu, Mn and O with their atomic percentage of 31.25, 12.64, and 56.11%, respectively, which are almost identical to the molar ratio of precursor. Further the elemental mapping (Fig. 1f) confirms the harmonized scattering of Cu, Mn and O.

The formation of metal glycolate and gas bubbles are playing a vital role for the construction of MCO microspheres. When added the metal precursor to EG solution, metal alkoxides were formed due to the coordination bonding interaction between the EG and metal cations (Cu(II) and Mn(II)).[27] Then, as-formed metal glycolate joins each other at elevated temperature and microspheres were formed caused by the van der Waals interactions. Besides, during the solvothermalysis, gas bubbles such as NH_3 and CO_2 will be produced by decomposition of urea at high temperature to afford more active sites.[39] As-formed metal alkoxides are less stable because of high energy and accumulate at the gas–liquid interface to minimize the interfacial energy.[38,39] At last, in the thermal treatment, gaseous molecules have been released from the precursor,[27] thus the microspheres were effectively achieved.

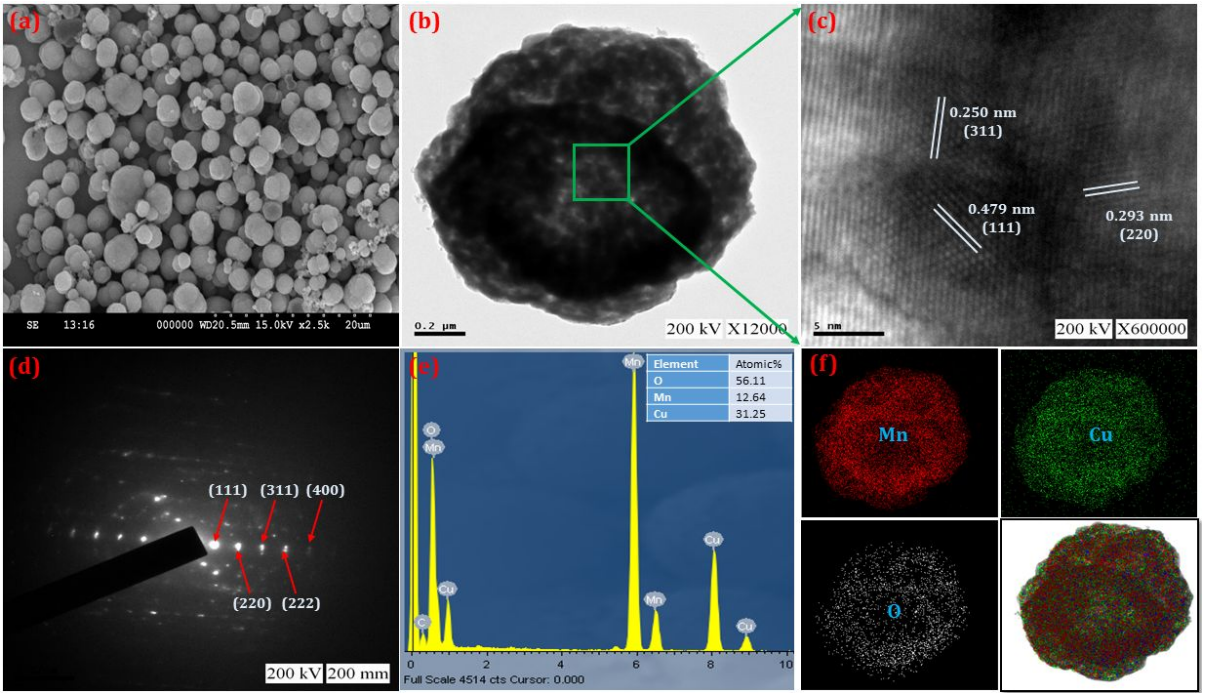

Fig. 1. FESEM (a), TEM image (b), HRTEM (c), SAED (d), EDX spectra (e) and elemental mapping (f) of MCO microspheres.

The crystallinity and phase pureness of MCO has been analyzed via X-ray diffraction (XRD) method and shown in Fig 2a. As-depicted in Fig 2a, MCO microspheres exhibited the characteristic diffraction peaks at 18.47, 30.39, 35.81, 37.46, 43.52, 47.66, 54, 57.58, 63.25, 66.51, 71.78, 74.86, 75.88, and 79.91°, which are corresponding to the (111), (220), (311), (222), (400), (331), (422), (511), (440), (531), (620), (533), (622), and (444) crystal planes of cubic Mn_2CuO_4

phase ([FM3-M]-Space group 227) (JCPDS no. 076-2296). This result confirms the formation of pure single-phase Mn_2CuO_4 without other possible impurities. FT-IR spectrum of MCO microspheres is shown in Fig. 2b. The vibration bands at 437 and 520 cm^{-1} were assigned to the stretching vibrations of Mn-O.[40] The bands at 556 and 618 cm^{-1} are corresponding to the stretching vibrations of Cu-O. Whereas, a couple of week intense peaks at 1103 cm^{-1} and 658 cm^{-1} are ascribed to Mn^{3+} stretching vibration in octahedral site, and linear units of CuO_2^{3-}, correspondingly.[41,42] In addition, the weak band at 1620 cm^{-1} and strong vibration at 3430 cm^{-1} are ascribed to the bending and stretching vibration mode of absorbed water.[42] Consequently, FT-IR results further confirming the formation of Mn_2CuO_4.

To explore the chemical composition and electronic state of elements XPS analysis was employed. Fig. 2c presents the survey scan of MCO, authorizes the presence of Mn, Cu, and O. Further, Mn 2p spectrum in Fig. 2e, the binding energies of 643, and 654.5 eV have been ascribed to the Mn $2p_{3/2}$ and Mn $2p_{1/2}$, correspondingly.[42] The calculated spin energy separation to be 11.5, coincide with earlier literature.[43] It can be further into four peaks. In the deconvoluted spectrum of Mn $2p_{3/2}$, the binding energies of 645.9 and 642.6 eV can be attributed to the presence of Mn^{4+} and Mn^{3+} species, correspondingly. Similarly, in the deconvoluted spectrum of Mn $2p_{1/2}$, the fitted peaks at 654.3, and 658.6 eV, allotted to Mn^{4+} and Mn^{3+}, correspondingly.[44] Further, the spectrum of Cu 2p (Fig. 2e) can be split into four peaks. The binding energies of 932.4 (Cu $2p_{3/2}$) and 952.3 eV (Cu $2p_{1/2}$) could be ascribed to the tetrahedrally coordinated Cu^+, whereas binding energies of 934.7 (Cu $2p_{3/2}$) and 955 eV (Cu $2p_{1/2}$) assigned to the octahedrally coordinated Cu^{2+}.[45] In addition to the major peaks, two satellite peaks were appeared at about 944.5 and 963.5 eV, agrees to the Cu $2p_{3/2}$ and Cu $2p_{1/2}$.[44] The spin-energy separation of Cu $2p_{3/2}$ and Cu $2p_{1/2}$ of around 20 eV,[46] thus confirming the presence of Cu^+ and Cu^{2+}. As depicted in Fig. 2f O1s spectrum can be fragmented into two peaks indicate existence of two different states of oxygen on the surface of MCO. The peaks at 529.68, and 531.75 eV due to the lattice oxygen (metal-oxygen bonding) (O^{2-}), and adsorbed oxygen (O_2^-/O^-).[44]

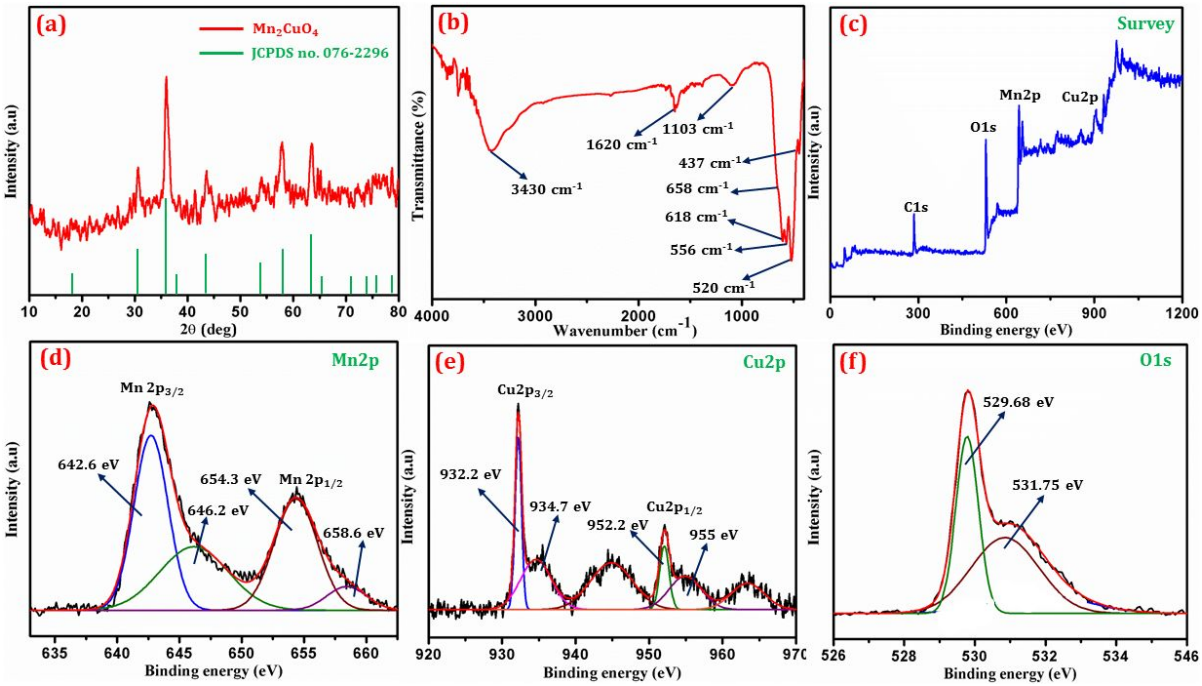

Fig. 2. Powder X-ray diffraction (a), FT-IR spectrum (b), XPS survey spectrum (c), Mn2p (d), Cu2p (e) and O1s (f) of MCO microspheres.

Electrochemical impedance spectral (EIS) studies

To explore the electron transfer (interfacial) behaviour of modified electrode, EIS measurements has been done (Fig. 3a). As depicts in Fig. 3a, Nyquist plots (impedance curve) of bare GCE (a), CuO/GCE (b) and MCO/GCE (c) were recorded in 0.1 M KCl in the presence of 5 mM $[Fe(CN)_6]^{3-/4-}$. The semicircle section of Nyquist plots is resulted by charge-transfer limitation, whereas the linear part is ascribed with diffusion-limited process.[47] The diameter of the semicircle reveals the charge transfer resistance of the respective electrode. The estimated impedance (R_{ct}) at bare GCE (a) is 86 Ω, indicating very low impedance. The semicircle diameter of the CuO/GCE (b), significantly increased, and the calculated charge transfer resistance to be 291 Ω, demonstrating that the CuO hindered the diffusion of the electrochemical probe. This is might be due to the semiconducting behaviour of CuO, is agree with earlier reports.[48] The charge transfer resistance (R_{ct}) value obtained at MCO/GCE (c) is decreased remarkably to 103 Ω, demonstrating that the electro transfer process at MCO microspheres is easier than CuO. The results validate that incorporation of Mn into CuO lattice greatly enhanced the ionic conductivity of MCO microspheres.

Electrocatalytic reduction of H_2O_2 at MCO/GCE

To assess the electrocatalytic performance of MCO/GCE towards the detection of H_2O_2, CVs have been performed in presence, and absence of H_2O_2. The Fig. 4b shows the CVs obtained for bare GCE (a), CuO/GCE (b), and MCO/GCE (c) in deoxygenated 0.05 M PBS (pH 7) absence (a'-c') and presence (a-c) of H_2O_2 (1 mM) with a scan rate of 50 mV s^{-1}. The bare GCE (a') did not shows any redox peaks due to fact that absence of redox species and demonstrates a very poor electrocatalytic activity towards 1 mM H_2O_2 (a), indicating that bare GCE is unable to sense H_2O_2. In absence of H_2O_2, the CuO/GCE (b'), and MCO/GCE (c'), displayed a pair of redox peaks corresponds to the Cu(I)/Cu(II) redox couple.[13] It should be noteworthy that the MCO/GCE (c'), exhibits a distinct redox peak over the CuO/GCE might be the intermetallic (between Mn and Cu) charge transfer, subsequently reformed the electronic structure of CuO in Mn_2CuO_4 can meaningfully enlightening electrocatalysis.[5] While adding the H_2O_2, a significant current response was observed at around -0.26 V for CuO/GCE, illuminating that CuO possess a substantial electrocatalytic ability towards H_2O_2 reduction.[34,36,37] As expected, MCO/GCE shows a distinct cathodic peak current at a peak potential of -0.19 V with dramatically enhanced current response, which is almost 7.6- fold higher than the current response received at CuO/GCE, owing to the synergistic effect.

From the survey, Cu(I)/Cu(II) redox couple is responsible for the electrochemical reduction of H_2O_2.[33] In the process of H_2O_2 reduction, O-O bond cleavage is the rate-determining step with an activation energy of 50 kcl mol^{-1}.[49] The superior electrochemical sensing performance of MCO can be endorsed by minimizing the energy barrier for the O-O cleavage by doping Mn. The less electron affinitive Mn can donate electrons to facilitate the electroreduction of H_2O_2.[49] Meanwhile Mn^{2+} (electronegativity is 1.3) is a strong electron donor than Cu^{2+} (electronegativity is 2.0),[50] thus the reaction rate is boosted by incorporation of Mn with Cu. Hence, Mn_2CuO_4 demonstrated superior catalytic activity towards electroreduction of H_2O_2 than CuO.

Further, the electrode kinetics of MCO/GCE, was studied via CV. The CVs were performed in 0.05 M PBS in presence of 1 mM H_2O_2 with variable sweep rates and shown in Fig. 3c. As evident, the cathodic response current grows with increasing scan rate from 20 to 200 mV s^{-1}. As-obtained response currents (I_{pc}) were linear dependence with the square root of the scan

rates ($v^{1/2}$) (Fig. 3d), designates that electrocatalytic reduction of H_2O_2 over the MCO/GCE is a diffusion-controlled electrode process, in analogous with earlier reports.[4]

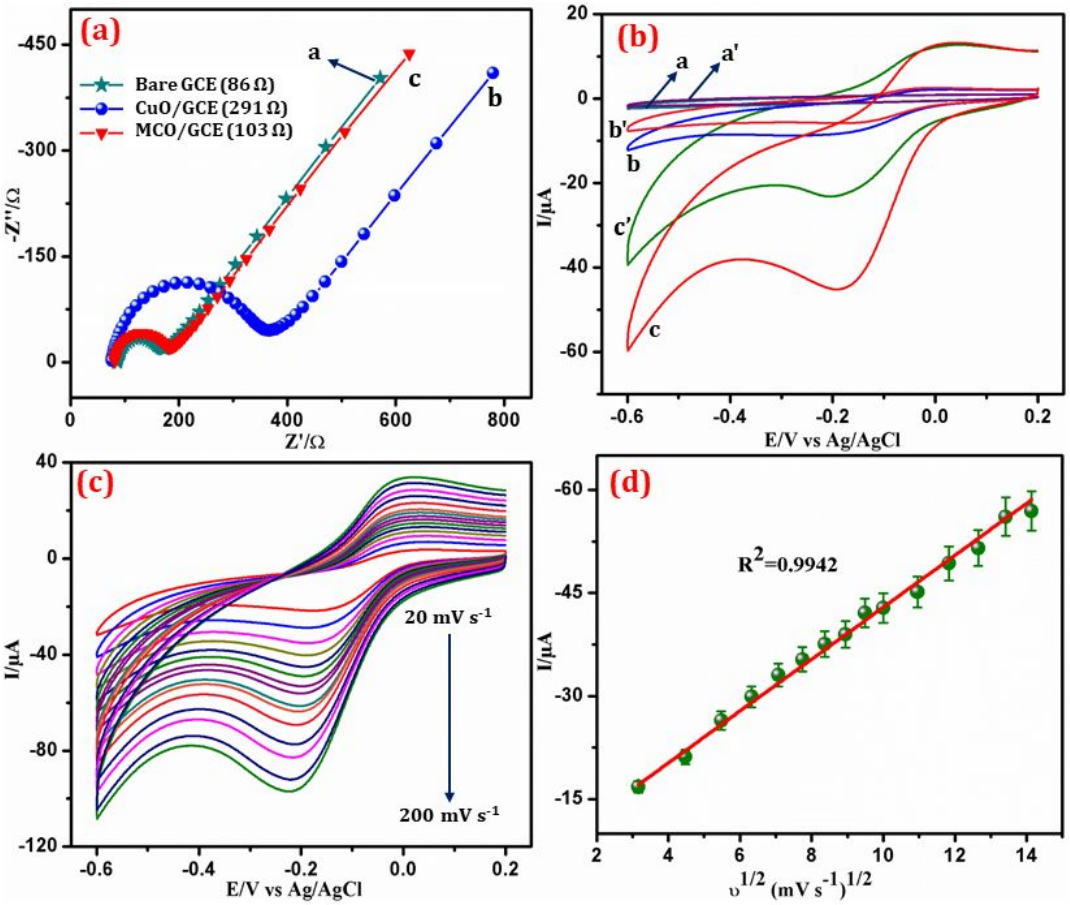

Fig. 3. (a) Impedance spectra of bare GCE (a), CuO/GCE (b), and MCO/GCE (c). (b) CVs of bare GCE, CuO/GCE, and MCO/GCE in 0.05 M PBS (pH 7) in the absence (denoted as a', b', c') and presence (denoted as a, b, c) of 1 mM H_2O_2 at a sweep rate of 50 mV s^{-1}. (c) CVs of MCO/GCE in 0.05 M PBS (pH 7) in the presence of 1 mM H_2O_2 with various a scan rates from 20 to 200 mV s^{-1}. (d) Linear fitting between the square root of the scan rate ($v^{1/2}$) and cathodic current response (I_{pc}) (n=3).

Amperometric determination of H_2O_2 on MCO modified electrode

The applied potential is an essential parameter for an amperometric sensor as it can influence the sensitivity of the developed sensor. In order to obtain an optimal assay potential for H_2O_2 detection; the amperometric measurements were carried out with MCO modified electrode at different applied potentials (0, -0.1, -0.2, -0.3, and -0.4 V). From Fig. 4a, the amperometric

response current towards H_2O_2 improved remarkably with increasing applied potential up to -0.2 V and found to be decreasing with further increment of applied potential. At most current response can be attained at an applied potential of -0.2 V, and it was elected as operating potential for amperometric H_2O_2 sensor.

Next, the amperometric measurement were performed to define the analytical performance of the sensor such, detection limit, dynamic range, and sensitivity of H_2O_2 detection on MCO/GCE. Fig. 4b illustrates the amperometric current response of MCO/RDE upon the cumulative injection of H_2O_2 in constantly stirred 0.05 M PBS (pH 7) at an operating potential of -0.2 V. Fig. 4c portrays the linear plot against the response current and concentration of H_2O_2 in the range of 36 nM to 9.3 mM and a correlation coefficient of 0.9945 (R^2). The detection limit, and assay sensitivity was estimated from the slope of the calibration curve, and found to be 13 nM (S/N=3), and 3.107 μA μM^{-1} cm^{-2}, correspondingly. The analytical performances of MCO modified electrode were comparable with the recently reported H_2O_2 sensors (Table 1). In evident from Table 1, the sensing performance of the MCO based sensor is either superior or in line with other reported sensors, by means of dynamic range, and detection limit. This excellent electrochemical sensing performance promoted from the rough surface and sphere-like structure and strong synergetic effect of Mn_2CuO_4 microspheres.

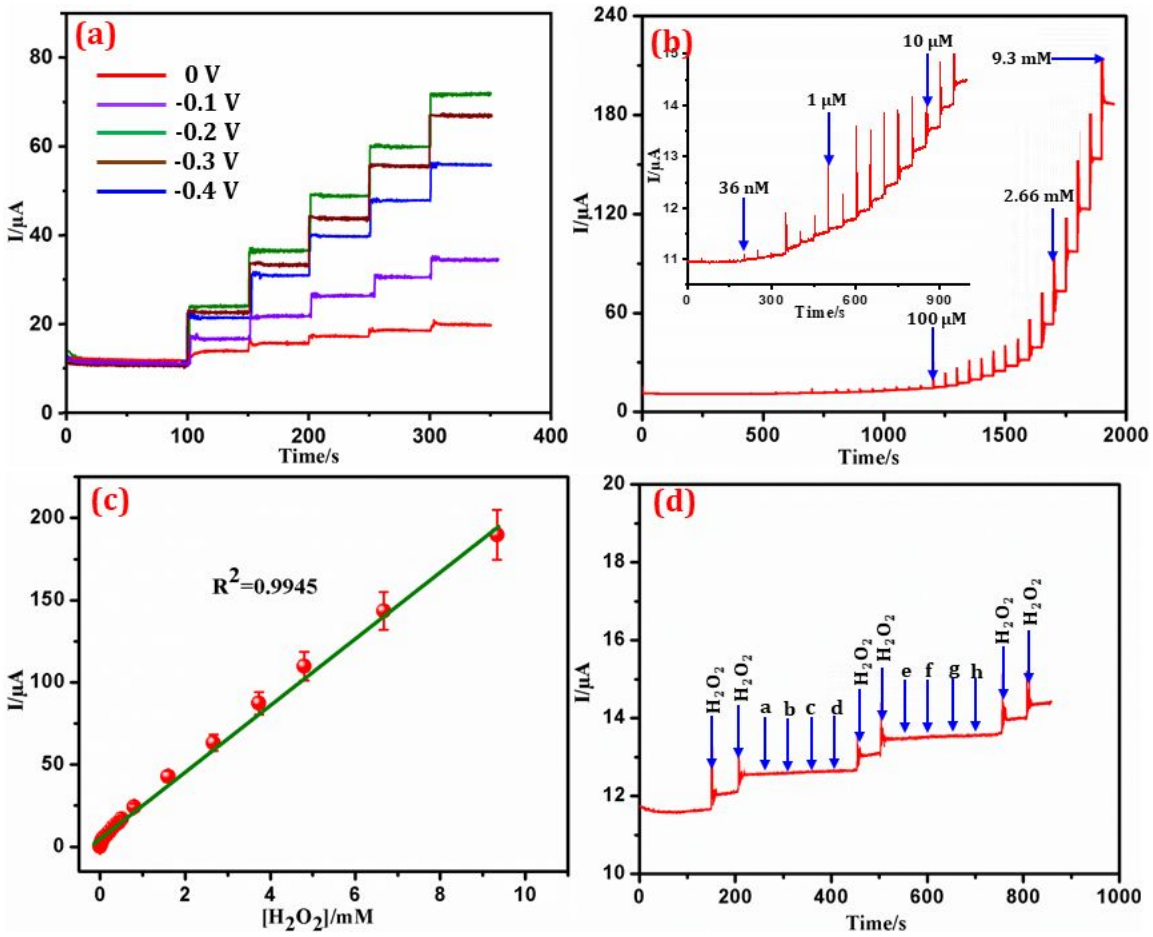

Fig. 4. (a) Amperometric current response of MCO/RDE at various operating potentials in 0.05 M PBS (pH 7) under consecutive injection of H_2O_2 (1 mM) (b) Amperometric current response of MCO/RDE on cumulative injection of H_2O_2 into 0.05 M PBS (pH 7) at operating potential of -0.2 V. (inset: current response of H_2O_2 at lower concentrations) (c) calibration plot of concentration of H_2O_2 vs amperometric current response (n=3). (d) Amperometric response of MCO/RDE on consecutive addition of 200 μM AA, DA, UA, glu, urea, L-cys, NaCl, and KCl with 100 μM H_2O_2.

Table. 1 Assessing the analytical parameters of MCO/RDE sensor over electrochemical H_2O_2 sensors

Electrode material	linear response (μM)	LOD (μM)	ref
Au@C-Co_3O_4	0.05-100 100 - 3000	0.019	3
Ag nanosheets	0.5-6000	0.17	4

Pt-Pd/CFME	0.5-3920	0.42	11
CuO@MnAl NSs	6-2200	0.126	13
RGO/Pt	0. 5-3475	0.2	14
MoS_2/Pt	1-100	0.686	15
Pt/PG	1-1477	0.5	20
Pt-DENs/CNTs	3-400	0.8	21
$CoFe_2O_4$	10-1200	2.5	28
$CoSn(OH)_6$	4-400	1	30
MnO_2	0.025-2	0.005	51
Mn_2CuO_4	0.036–9300	0.013	This work

Au@C-Co_3O_4−Au nanoparticles encapsulated carbon/cobalt oxide; CFME−carbon fiber microelectrode; RGO/Pt−reduced graphene oxide/platinum nanoparticles; PG-porous graphene; Pt-DENs/CNTs−Pt nanoclusters/carbon nanotubes

The selectivity is a major concern in non-enzymatic H_2O_2 biosensors; and limiting the applicability of a developed sensor in day-today practice. The influence of current response of electroactive species such, ascorbic acid (AA), dopamine (DA), uric acid (UA), glucose (glu), urea, L-cysteine (L-cys), KCl, and NaCl on the MCO/GCE for H_2O_2 sensing were assessed by amperometry, presented in Fig. 4d. It can be seen that the addition of 200 μM of interferents did not produce any significant current response signal and does not affect the current response of 100 μM H_2O_2. These results authenticate that the developed biosensor can selectively detect H_2O_2 in coexistence of interfering species at high concentration. Thus, good selectivity is validated with high precision.

In order to explore the reliability of the sensor, the MCO/GCE was kept in air at room temperature for one month, and CV response current of such electrode were noted every 24 h. The electrode preserved 94.6% of its original response current towards 1 mM H_2O_2 over 30 days (Fig 5a). These results advocate the storage stability of the proposed MCO/GCE based H_2O_2. Then to evaluate the repeatability of the sensor, current response of ten repeated CVs was performed in 0.05 PBS (pH 7) with1 mM H_2O_2. As shown Fig. 5b, H_2O_2 reduction peak currents maintained around 96.9% of their primary current values with a relative standard deviation (RSD) of about 1.09% for the MCO modified electrode, revealing that the electrodes are repeatable. The

reproducibility of the MCO/GCE was studied by CV response towards 1 mM H_2O_2 carried out with six different MCO modified electrodes fabricated via constant protocol. The results were given in Fig. 5c, no obvious decrease in reduction peak current of H_2O_2, the results imply that the modified electrodes have good reproducibility, where the calculated RSD value is about 1.31%. Finally, the MCO/GCE revealed admirable stability, repeatability, and reproducibility to determine H_2O_2, which are essential features for a sensor in real time applications.

Determination of endogenous H_2O_2 released from RAW 264.7 cells

The cultured RAW 264.7 cells were transferred into PBS (pH 7) and amperometric measurements were performed at an operating potential of -0.2 V. The addition of CHAPS when to the buffer (i.e., in absence of cells) did not produces any current response (red). As shown in Fig. 5d, the RAW 264.7 cells in absence of CHAPS does not produce any response current (blue), indicating that the cells require stimulant to produce H_2O_2. However, injection of 0.5 μM CHAPS into electrolyte containing 2×10^6 RAW 264.7 cells, the cathodic current significantly increased (green), and the response current was corresponding to the H_2O_2 produced by RAW 264.7 cells upon stimulation with CHAPS. In addition, the subsequent addition of catalase (H_2O_2 scavenger) to the test sample resulted in drop of response current produced by injecting CHAPS to the RAW 264.7 cells.[19] The measured response current (blue curve) was about 0.87 μA, equivalent to 180 nM H_2O_2 (calculated from analytical curve (Fig.4c)). Furthermore, the amount H_2O_2 released per cell was calculated about 9×10^{-14} M, which is coincide with earlier literature.[52,53,54] The results revealed here validate that the established Mn_2CuO_4 based sensor can be used in real-time detection of extra-cellular H_2O_2 secreted by living cells.

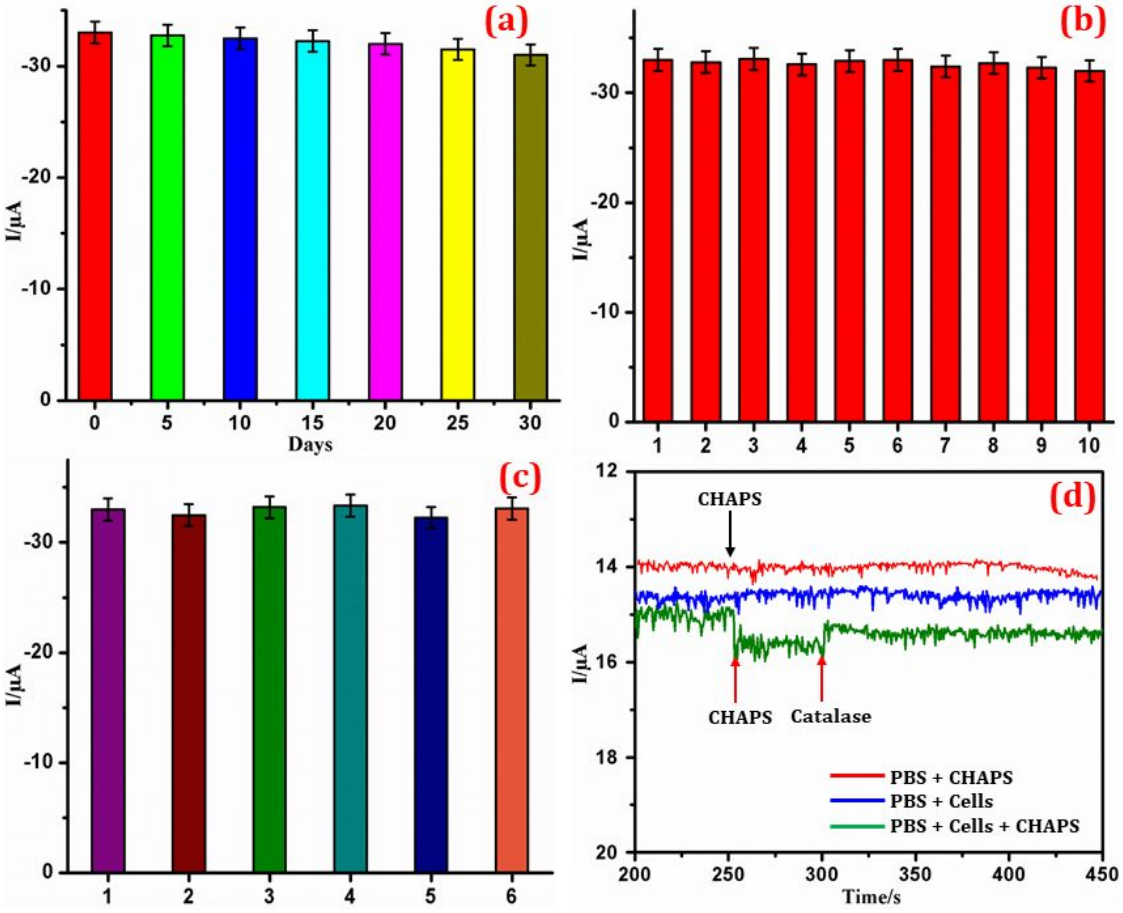

Fig. 5. (a) Response current of MCO/GCE towards 1 mM H_2O_2 for one month (n=3). (b) Response current of 10 repetitive CVs of a same MCO/GCE in 0.05 M PBS (pH 7) with 1 mM H_2O_2 (n=3). (c) Response current of six different MCO/GCE prepared in identical protocol in 0.05 M PBS (pH 7) with 1 mM H_2O_2 (n=3). (d) Amperometric current response of MCO/RDE in 0.05 M PBS (pH 7) having RAW 264.7 cells (2×10^6 cells) in absence (a) and presence (b) of CHAPS and catalase.

CONCLUSION

In brief, we proposed a high sensitive, selective, enzymeless electrochemical biosensor for H_2O_2 detection based on Mn_2CuO_4 (MCO) as an electrocatalyst. The microsphere-like MCO was prepared by a facile and efficient solvothermal strategy. Electrochemical impedance spectral studies obvious that the introduction of manganese into copper oxide lattice significantly improved the ionic conductivity, thus can obtain excellent electrochemical sensing performance. The electrocatalytic sensing studies demonstrates that the MCO modified electrode exhibited admirable electrochemical performance. Owing to the lower electron affinity of Mn; it acts as an

electron donor to luxuries the electroreduction of H_2O_2, thus the reaction rate is boosted by incorporation of Mn with Cu. Owing the unique microsphere-like structure and admirable elemental synergy of MCO, the biosensor based on MCO was achieved a working range of 36 nM to 9.3 mM with a detection limit of 13 nM towards H_2O_2. The biosensor can further realize *in-situ* detection of trace-level H_2O_2 secreted from Raw 264.7 cells. These results designate the probable utility of the sensor in various fields of bioanalytical chemistry. All these unique features of Mn_2CuO_4, make it an intriguing candidate to development an efficient electrochemical biosensor for point-of-care application.

ACKNOWLEDGEMENTS

The authors gratefully acknowledge the financial support of the Ministry of Science and Technology, Taiwan through contract no. MOST 107-2113-M-027-005-MY3.

ASSOCIATED CONTENT

Supplementary information

Materials and methods, Preparation of MCO modified electrode and RAW 264.7 cells for real time detection of H_2O_2

AUTHOR INFORMATION

Corresponding Author: *Shen-Ming Chen, Fax: +886227025238, Tel: +886227017147,
E-mail: smchen78@ms15.hinet.net

Conflicts of interest

There are no conflicts to declare.

REFERENCES

[1] Li, C., Wu, R., Zou, J., Zhang, T., Zhang, S., Zhang, Z., Ling, X. MNPs@ anionic MOFs/ERGO with the size selectivity for the electrochemical determination of H_2O_2 released from living cells. *Biosens. Bioelectron*. **2018**, 116, 81–88.

[2] Zhang, R., Chen, W. Recent advances in graphene-based nanomaterials for fabricating electrochemical hydrogen peroxide sensors. *Biosens. Bioelectron*. **2017,** 89, 249–268.

[3] Dai, H., Chen, Y., Niu, X., Pan, C., Chen, H., Chen, X. High-performance electrochemical biosensor for nonenzymatic H_2O_2 sensing based on Au@C-Co_3O_4 heterostructures. *Biosens. Bioelectron*. **2018,** 118, 36–43.

[4] Ma, B., Kong, C., Hu, X., Liu, K., Huang, Q., Lv, J., Yang, S. A sensitive electrochemical nonenzymatic biosensor for the detection of H_2O_2 released from living cells based on ultrathin concave Ag nanosheets. *Biosens. Bioelectron*. **2018,** 106, 29–36.

[5] Asif, M., Liu, H., Aziz, A., Wang, H., Wang, Z., Ajmal, M., Liu, H. Core-shell iron oxide-layered double hydroxide: High electrochemical sensing performance of H_2O_2 biomarker in live cancer cells with plasma therapeutics. *Biosens. Bioelectron*. **2017,** 97, 352–359.

[6] Bai, Z., Li, G., Liang, J., Su, J., Zhang, Y., Chen, H., Huang, Y., Sui, W., Zhao, Y., Non-enzymatic electrochemical biosensor based on Pt NPs/RGO-CS-Fc nano-hybrids for the detection of hydrogen peroxide in living cells. *Biosens. Bioelectron*. **2016**, 82, 185–194.

[7] Ding, N., Yan, N., Ren, C., Chen, X. Colorimetric determination of melamine in dairy products by Fe_3O_4 magnetic nanoparticles H_2O_2 ABTS detection system, *Anal. Chem.* **2010,** 82, 5897–5899.

[8] Chinnasamy, R., Rao, G. M. Synthesis and electrocatalytic properties of manganese dioxide for non-enzymatic hydrogen peroxide sensing, *Mater. Sci. Semicond. Process.* **2015,** 31, 709–714.

[9] Tarvin, M., McCord, B., Mount, K., Sherlach, K., Miller, M. L. Optimization of two methods for the analysis of hydrogen peroxide: high performance liquid chromatography with fluorescence detection and high-performance liquid chromatography with electrochemical detection in direct current mode, *J. Chromatogr. A* **2010,** 1217, 7564–7572.

[10] Dickinson, B. C., Chang, C. J. A targetable fluorescent probe for imaging hydrogen peroxide in the mitochondria of living cells, *J. Am. Chem. Soc*. **2008,** 130, 9638–9639.

[11] Li, H., Zhao, H., He, H., Shi, L., Cai, X., Lan, M. Pt-Pd bimetallic nanocoral modified carbon fiber microelectrode as a sensitive hydrogen peroxide sensor for cellular detection. *Sens Actuators B Chem.* **2018,** 260, 174–182.

[12] Liu, J., Bo, X., Yang, J., Yin, D., Guo, L. One-step synthesis of porphyrinic iron-based metal-organic framework/ordered mesoporous carbon for electrochemical detection of hydrogen peroxide in living cells. *Sens Actuators B Chem.* **2017,** 248, 207–213.

[13] Asif, M., Haitao, W., Shuang, D., Aziz, A., Zhang, G., Xiao, F., Liu, H. Metal oxide intercalated layered double hydroxide nanosphere: With enhanced electrocatalyic activity towards H_2O_2 for biological applications. *Sens Actuators B Chem.* **2017,** 239, 243–252.

[14] Zhang, Y., Bai, X., Wang, X., Shiu, K. K., Zhu, Y., Jiang, H. Highly Sensitive Graphene−Pt Nanocomposites Amperometric Biosensor and Its Application in Living Cell H_2O_2 Detection. *Anal. Chem*. **2014**, 86, 9459−9465.

[15] Zhou, J. X., Tang, L. N., Yang, F., Liang, F. X., Wang, H., Li, Y. T., Zhang, G. J. MoS_2/Pt nanocomposite-functionalized microneedle for real-time monitoring of hydrogen peroxide release from living cells. *Analyst*, **2017**, 142, 4322.

[16] Tahernejad-Javazmi, F., Shabani-Nooshabadi, M., Karimi-Maleh, H. Analysis of glutathione in the presence of acetaminophen and tyrosine via an amplified electrode with MgO/SWCNTs as a sensor in the hemolyzed erythrocyte. *Talanta* **2018,** 176, 208-213.

[17] Akbarian, Y., Shabani-Nooshabadi, M., Karimi-Maleh, H. Fabrication of a new electrocatalytic sensor for determination of diclofenac, morphine and mefenamic acid using synergic effect of NiO-SWCNT and 2, 4-dimethyl-N/-[1-(2, 3-dihydroxy phenyl) methylidene] aniline. *Sens Actuators B Chem.* **2018**, 273, 228-233.

[18] Tahernejad-Javazmi, F., Shabani-Nooshabadi, M., Karimi-Maleh, H. Gold nanoparticles and reduced graphene oxide-amplified label-free DNA biosensor for dasatinib detection. *New J. Chem.* **2018**, 42, 16378-16383.

[19] Dou, B., Yang, J., Yuan, R., Xiang, Y. Trimetallic Hybrid Nanoflower-Decorated MoS2 Nanosheet Sensor for Direct in Situ Monitoring of H_2O_2 Secreted from Live Cancer Cells. *Anal. Chem*. **2018**, 90, 5945−5950.

[20] Liu, J., Bo, X., Zhao, Z., Guo, L. Highly exposed Pt nanoparticles supported on porous graphene for electrochemical detection of hydrogen peroxide in living cells. *Biosens. Bioelectron*. **2015**, 74, 71–77.

[21] Liu, J. X., Ding, S. N. Non-enzymatic amperometric determination of cellular hydrogen peroxide using dendrimer-encapsulated Pt nanoclusters/carbon nanotubes hybrid composites modified glassy carbon electrode. *Sens Actuators B Chem.* **2017,** 251, 200–207.

[22] Zhu, C., Yang, G., Li, H., Du, D., Lin, Y. Electrochemical Sensors and Biosensors Based on Nanomaterials and Nanostructures. *Anal. Chem*. **2015**, 87, 230−249.

[23] Chen, W., Cai, S., Ren, Q. Q., Wen, W., Zhao, Y. D. Recent advances in electrochemical sensing for hydrogen peroxide: a review. *Analyst,* **2012**, 137, 49.

[24] Zhang, Y., Li, L., Su, H., Huang, W., Dong, X. Binary metal oxide: advanced energy storage materials in supercapacitors. *J. Mater. Chem. A*, **2015**, 3, 43.

[25] Yuan, C., Wu, H. B., Xie, Y., Lou, X. W. Mixed Transition-Metal Oxides: Design, Synthesis, and Energy-Related Applications. *Angew. Chem. Int. Ed.* **2014**, 53, 1488 – 1504.

[26] Wu, Z. L., Li, C. K., Zhu, F. W., Liao, S., Yu, J. G., Yang, H., Chen, X. Q. Binary cobalt and manganese oxides: Amperometric sensing of hydrogen peroxide. *Sens Actuators B Chem.* **2017,** 253, 949–957.

[27] Balasubramanian, P., Balamurugan, T. S. T., Chen, S. M., Chen, T. W. Simplistic synthesis of ultrafine $CoMnO_3$ nanosheets: An excellent electrocatalyst for highly sensitive detection of toxic 4-nitrophenol in environmental water samples. *J Hazard Mater* **2019,** 361, 123–133.

[28] Vasuki, K., Babu, K. J., Sheet, S., Siva, G., Kim, A. R., Yoo, D. J. Amperometric hydrogen peroxide sensor based on the use of $CoFe_2O_4$ hollow nanostructures. *Microchim Acta* **2017,** 184, 2579–2586.

[29] Liu, W., Zhou, Z., Yin, L., Zhu, Y., Zhao, J., Zhu, B., Wang, L. A novel self-powered bioelectrochemical sensor based on $CoMn_2O_4$ nanoparticle modified cathode for sensitive and rapid detection of hydrogen peroxide. *Sens Actuators B Chem.* **2018,** 271, 247–255.

[30] Shu, Y., Li, B., Xu, Q., Gu, P., Xiao, X., Liu, F., Hu, X. Cube-like $CoSn(OH)_6$ nanostructure for sensitive electrochemical detection of H2O2in human serum sample. *Sens Actuators B Chem.* **2017,** 241, 528–533.

[31] Zhu, L., Zhang, Y., Xu, P., Wen, W., Li, X., Xu, J. PtW/MoS_2 hybrid nanocomposite for electrochemical sensing of H_2O_2 released from living cells. *Biosens. Bioelectron*. **2016,** 80, 601–606.

[32] Song, H., Ni, Y., Kokot, S. A novel electrochemical sensor based on the copper-doped copper oxide nano-particles for the analysis of hydrogen peroxide. *Colloids Surf A Physicochem Eng Asp.* **2015,** 465, 153–158.

[33] Antink, W. H., Choi, Y., Seong, K. D., Piao, Y. Simple synthesis of CuO/Ag nanocomposite electrode using precursor ink for non-enzymatic electrochemical hydrogen peroxide sensing. *Sens Actuators B Chem.* **2018,** 255, 1995–2001.

[34] Gao, P., Liu, D. Facile synthesis of copper oxide nanostructures and their application in non-enzymatic hydrogen peroxide sensing. *Sens Actuators B Chem.* **2015,** 208, 346–354.

[35] Ping, J., Ru, S., Fan, K., Wu, J., Ying, Y. Copper oxide nanoparticles and ionic liquid modified carbon electrode for the non-enzymatic electrochemical sensing of hydrogen peroxide. *Microchim Acta* **2010**, 171, 117–123.

[36] Song, M. J., Hwang, S. W., Whang, D. Non-enzymatic electrochemical CuO nanoflowers sensor for hydrogen peroxide detection. *Talanta* **2010,** 80, 1648–1652.

[37] Zhang, L., Li, H., Ni, Y., Li, J., Liao, K., Zhao, G. Porous cuprous oxide microcubes for non-enzymatic amperometric hydrogen peroxide and glucose sensing. *Electrochem. Commun.* **2009,** 11, 812–815.

[38] You, H., Zhang, L., Jiang, Y., Shao, T., Li, M., Gong, J. Bubble-supported engineering of hierarchical $CuCo_2S_4$ hollow spheres for enhanced electrochemical performance. *J. Mater. Chem. A.* **2017**, 6, 5265-5270.

[39] Hu, L., Zhong, H., Zheng, X., Huang, Y., Zhang, P., Chen, Q. $CoMn_2O_4$ Spinel Hierarchical Microspheres Assembled with Porous Nanosheets as Stable Anodes for Lithium-ion Batteries. *Sci. Rep.* **2012**, 2, 986.

[40] Poienar, M., Banica, R., Sfirloaga, P., Ianasi, C., Mihali, C. V., Vlazan, P. Microwave-assisted hydrothermal synthesis and catalytic activity study of crednerite-type $CuMnO_2$ materials. *Ceram. Int.* **2018,** 44, 6157–6161.

[41] Wang, L., Arif, M., Duan, G., Chen, S., Liu, X. A high performance quasi-solid-state supercapacitor based on CuMnO2 nanoparticles. *J. Power Sources* **2017,** 355, 53-61.

[42] Benreguia, N., Barnabé, A., Trari, M. Preparation and characterization of the semiconductor $CuMnO_2$ by sol-gel route. *Mater Sci Semicond Process.* **2016,** 56, 14–19.

[43] Li, Q., Yin, L., Li, Z., Wang, X., Qi, Y., Ma, J. Copper Doped Hollow Structured Manganese Oxide Mesocrystals with Controlled Phase Structure and Morphology as

Anode Materials for Lithium Ion Battery with Improved Electrochemical Performance. *ACS Appl. Mater. Interfaces* **2013**, 5, 10975−10984.

[44] Liu, T., Yao, Y., Wei, L., Shi, Z., Han, L., Yuan, H., Sun, C. Preparation and Evaluation of Copper−Manganese Oxide as a High-Efficiency Catalyst for CO Oxidation and NO Reduction by CO. *J. Phys. Chem. C* **2017**, 121, 12757−12770.

[45] Karmakar, A., Srivastava, S. K. Interconnected Copper Cobaltite Nanochains as Efficient Electrocatalysts for Water Oxidation in Alkaline Medium. *ACS Appl. Mater. Interfaces* **2017**, 9, 22378−22387.

[46] Chen, H. Y., Lin, Y. C., Lee, J. S. Crednerite-$CuMnO_2$ thin films prepared using atmospheric pressure plasma annealing. *Appl Surf Sci.* **2015**, 338, 113–119.

[47] Liu, Y., Shang, T., Liu, Y., Liu, X., Xue, Z., Liu, X. Highly sensitive platinum nanoparticles-embedded porous graphene sensor for monitoring ROS from living cells upon oxidative stress. *Sens Actuators B Chem.* **2018,** 263, 543–549.

[48] Wang, M. F., Huang, Q. A., Li, X. Z., Wei, Y. Mesoporous CuO: Alternative enzyme-free glucose sensing structure with excellent kinetics of electrode process. *Anal. Methods*, **2012**, 4, 3174–3179.

[49] Cheng, K., Yang, F., Wang, G., Yin, J., Cao, D. Facile synthesis of porous $(Co,Mn)_3O_4$ nanowires freestanding on a Ni foam and their catalytic performance for H_2O_2 electroreduction. *J. Mater. Chem. A*, **2013**, 1, 1669.

[50] Gordy, W., Thomas, W. O., Electronegativities of the Elements. *J. Chem. Phys*., *1956*, 24, 439–444.

[51] Shu, Y., Xu, J., Chen, J., Xu, Q., Xiao, X., Jin, D., Hu, X. Ultrasensitive electrochemical detection of H_2O_2 in living cells based on ultrathin MnO_2 nanosheets. *Sens Actuators B Chem.* **2017**, 252, 72-78.

[52] Li, Z., Xin, Y., Wu, W., Fu, B., Zhang, Z. Topotactic Conversion of Copper(I) Phosphide Nanowires for Sensitive Electrochemical Detection of H_2O_2 Release from Living Cells. *Anal. Chem*. ***2016***, 88, 7724−7729.

[53] Balamurugan, T. S. T., Mani, V., Hsieh, C. C., Huang, S. T., Peng, T. K., Lin, H. Y. Real-time tracking and quantification of endogenous hydrogen peroxide production in living cells using graphenated carbon nanotubes supported Prussian blue cubes. *Sens Actuators B Chem.* **2018,** 257, 220–227.

[54] Wang, N., Han, Y., Xu, Y., Gao, C., Cao, X. Detection of H_2O_2 at the Nanomolar Level by Electrode Modified with Ultrathin AuCu Nanowires. Anal. Chem. **2015**, 87, 457−463.

Table of Contents